Fermi National Accelerator Laboratory

FERMILAB-Pub-92/068

Slow Head-Tail Instability in a Proton Synchrotron

S. A. Bogacz

Fermi National Accelerator Laboratory
P.O. Box 500, Batavia, Illinois 60510

March 1992

Submitted to *Phys. Rev. A.*

Operated by Universities Research Association Inc. under Contract No. DE-AC02-76CHO3000 with the United States Department of Energy

SLOW HEAD-TAIL INSTABILITY IN A PROTON SYNCHROTRON

S.A. Bogacz

Accelerator Physics Department,
Fermi National Accelerator Laboratory*
P.O. Box 500, Batavia, IL 60510

February 1992

Presented study is motivated by a coherent betatron instability observed in the Tevatron. Here, a simple analytic model based on the Sacherer's formalism is extended to describe the slow head-tail instability. The so-called plane wave model of the transverse modes allows one to link different growth-time scales with the specific contributions to the transverse coupling impedance. As a result of this formalism the effective impedance, written in terms of the convolution of the beam spectrum and the relevant contribution to the coupling impedance, is evaluated explicitly via contour integration using Cauchy's integral theorem. Finally, a closed analytic formula describing the growth time vs chromaticity is obtained in the case of an arbitrary head-tail mode driven by a general peaked impedance. This result is in close agreement with similar calculation done in the framework of a more realistic Vlasov equation-based "air bag" model. Our formalism was tested numerically in case of the Tevatron's instability. Predicted values of the characteristic growth-times for various modes are in close agreement with the observed ones.

---

*Operated by the Universities Research Association, Inc., under a contract with the U.S. Department of Energy

INTRODUCTION – COHERENT BETATRON INSTABILITY

In the next few sections, a systematic analytic description of the slow head-tail instability will be presented. It yields a closed expression describing the characteristic growth-time of a given mode vs chromaticity. Finally, numerical example (in case of the Tevatron) shows a very good agreement between the measured values of the instability growth-times and the ones predicted on the basis of our model.

Here, we consider a case where both longitudinal and transverse oscillations are coupled through a finite chromaticity, ξ , according to the following relationship

$$\Delta\nu = \xi \frac{\Delta p}{p}, \tag{1.1}$$

where $\Delta\nu$ is the betatron tune shift and Δp is the longitudinal momentum deviation measured with respect to the synchronous particle (Δp defines position of a given particle within the bunch). One can consider a single particle initially at the "head" of the bunch ($\Delta p = 0$); its betatron tune matches the one of the synchronous particle. We also assume that both particles have initially the same betatron phases. Since the particle is undergoing synchrotron oscillations, while it is moving towards the "tail" of the bunch it lags in the betatron phase behind the synchronous particle ($\Delta\nu < 0$). After half of the synchrotron period the phase lag, χ, reaches maximum and the particle continues moving back towards the "head" of the bunch regaining previously lost phase. When a full synchrotron oscillation is completed the initial phase matching is recovered.

One can simply express the accumulated phase-lag in terms of the arrival time off-set, τ, (measured with respect to the synchronous particle) as follows

$$\chi = \frac{\xi}{\eta} \omega_0 \tau , \tag{1.2}$$

where ω_0 is the revolution frequency and η is the frequency dispersion function ($\eta < 0$ below the transition). Following an intuitive model of the head-tail instability proposed by Sacherer[1] we will assume that the amplitude of the transverse beam oscillation (related to the pick-up monitor signal) is a superposition of a standing plane wave (with the number of internal nodes defining the longitudinal mode index ℓ) and a propagating part describing previously discussed betatron phase lag/gain process (due to the finite chromaticity). The amplitude signal can be written as

$$A_\ell(\tau,k) = P_\ell(\tau)\, e^{i\omega_\xi\tau + 2\pi ik\nu}, \tag{1.3}$$

where $\omega_\xi = \frac{\xi}{\eta}\omega_0$ and k denotes the revolution number. Here the standing wave profile is modelled by simple harmonic functions

$$P_\ell(\tau) = \begin{cases} \cos[(\ell + 1)\,\pi\tau/2\hat{\tau}] & \ell \text{ even} \\ \sin[(\ell + 1)\,\pi\tau/2\hat{\tau}] & \ell \text{ odd} \end{cases}, \tag{1.4}$$

where $2\hat{\tau}$ is the bunch length (in units of time).

One can easily find the power spectrum of the transverse beam signal by taking the Fourier transform of Eq.(1.3)

$$A_\ell(\omega,k) = P_\ell(\omega - \omega_\xi)\; e^{2\pi ik\nu} \tag{1.5}$$

where

$$P_\ell(\omega) = \mathsf{F}\,\{P_\ell(\tau)\}\ .$$

One can see, that the beam spectrum is shifted by ω_ξ due to the presence of the propagating wave component. Periodicity given by the revolution period, $2\pi/\omega_o$, yields the discrete frequency spectrum with spacing ω_o. The envelope of the power spectrum is defined as

$$h_\ell(\omega) = |P_\ell(\omega)|^2$$

and is sampled by the frequencies (1.6)

$$\omega_p = (p + \nu)\omega_o$$

where p is an integer.

The explicit form of the power spectrum is given by the following expression[3]

$$h_\ell(\omega) = \frac{4}{\pi^2} (\ell + 1) \frac{1 + (-1)^\ell \cos(2\omega\hat{\tau})}{[(2\omega\hat{\tau}/\pi)^2 - (\ell + 1)^2]^2} , \tag{1.7}$$

which will serve as a spectral density function in evaluation of the averaged transverse self-force driving specific slow head-tail modes.

2. SINGLE PARTICLE DYNAMICS

Following Sacherer's argument[1] one can generalize a simple equation of motion describing a wake field driven coherent betatron motion of a coasting beam to model the head-tail instability of the bunched beam. A simple dipole oscillation of the coasting beam as a whole is governed by the following equation

$$\ddot{x} + (\nu\omega_o)^2 x = i \frac{e\beta}{\gamma m_o} \frac{Z_\perp I}{2\pi R} x . \tag{2.1}$$

Here x is the transverse displacement, $Z_\perp$ denotes the transverse coupling impedance, I is the total beam current and R is the machine radius. The following approach assumes ad hoc existence of a given head-tail mode, ℓ, previously described by Eqs.(1.3) and (1.4), by imposing specific periodic dependence of the betatron motion with respect to the longitudinal position, τ. This dependence is given by the following formula

$$x^\ell(t,\tau) = e^{i\Omega_\ell t} \sum_{p=-\infty}^{\infty} x_p^\ell \exp(\pi(\ell + 1)p\tau/2\hat{\tau}) , \tag{2.2}$$

where Ω_ℓ is the coherent frequency. The above expression imposes $(\ell + 1)$-fold periodicity on the betatron amplitude along the bunch.

In a case of a bunched beam the wake field experienced by a test particle at the position τ is now given by the following convolution of the transverse impedance and the normalized beam spectrum, ρ

$$V^\ell(\tau) = \omega_o \sum_{p=-\infty}^{\infty} Z_\perp(\omega_p)\, \rho^\ell(\omega_p - \omega_\xi)\, e^{\,i\omega_o\tau p} \quad , \tag{2.3}$$

where the beam spectrum for a given mode is defined as follows

$$\rho^{\ell}(\omega) = \frac{h^{\ell}(\omega)}{\sum_{p=-\infty}^{\infty} h^{\ell}(\omega_p)} \quad . \tag{2.4}$$

The deflecting transverse wake force acting on the particle is a sum of the wakes generated by all the particles in the bunch, which are ahead of the test particle (causality); it also includes long range wakes left from all the preceding turns. The last feature is explicitly built into the definition of $V^{\ell}(\tau)$, given by Eq.(2.3). Resulting transverse wake force is conveniently expressed by the following integral

$$F^{\ell}(\tau) = i\,\frac{e\beta}{\gamma m_o}\;\frac{I_o}{2\hat{\tau}c}\int_{\tau}^{\hat{\tau}} d\tau'\; V^{\ell}(\tau')\, h^{\ell}(\tau') \quad . \tag{2.5}$$

Substituting the above expression in the RHS of Eq.(2.1) and replacing x by Eq.(2.2) one obtains a complete equation of motion for the ℓ-th head-tail mode. Applying the following orthogonality identity

$$\frac{1}{2\hat{\tau}}\int_{-\hat{\tau}}^{\hat{\tau}} d\tau'\; \exp(\pi(\ell+1)(p - p')\tau'/2\hat{\tau}) = (\ell + 1)\,\delta_{p',p} \quad , \tag{2.6}$$

one can carry out the integration in Eq.(2.5). The resulting decoupled equation of motion for a single Fourier component is given by

$$[(\nu\omega_o)^2 - \Omega_{\ell}{}^2 - i\,\frac{e\beta}{\gamma m_o}\;\frac{I_o}{2\hat{\tau}c}\;\frac{1}{\ell + 1}\sum_{p'=-\infty}^{\infty} Z_{\perp}(\omega_{p'})\,\rho^{\ell}(\omega_{p'} - \omega_{\xi})\,]\,x^{\ell}_p = 0 \quad . \tag{2.7}$$

Assuming a nontrivial solution for x^{ℓ}_p yields explicit formula defining coherent frequency of the ℓ-th mode. Its imaginary part (with the negative sign) represents the inverse growth-time and is expressed by the following formula

$$\frac{1}{\tau^{\ell}} = - \frac{ce\beta I_o}{4\pi E v} \, \mathrm{Re}\, \mathcal{Z}^{\ell}_{\mathrm{eff}} \ , \tag{2.8}$$

where $E = \gamma m_o c^2$ is the total energy and $\mathcal{Z}^{\ell}_{\mathrm{eff}}$ is the effective impedance defined as follows

$$\mathcal{Z}^{\ell}_{\mathrm{eff}} = \frac{2\pi}{\ell + 1} \frac{1}{2\omega_o \hat{\tau}} \sum_{p' = -\infty}^{\infty} Z_{\perp}(\omega_{p'}) \, \rho^{\ell}(\omega_{p'} - \omega_{\xi}) \quad . \tag{2.9}$$

The above result can be compared with the growth-time obtained in the framework of the Vlasov equation-based description of the slow head-tail instability. The so-called "air bag" model[3] assumes δ-like shell structure of the longitudinal phase-space, which serves as the equilibrium density distribution function (on top of which various head-tail modes are constructed as small fluctuations of the particle density). The resulting formula has exactly the same generic form as given by Eq.(2.8) with the effective impedance introduced as an average over different set of spectral density functions; namely the Bessel functions of the first kind. This average is given explicitly as follows[5]

$$\mathcal{Z}^{\ell}_{\mathrm{eff}} = \sum_{p'=-\infty}^{\infty} Z_{\perp}(\omega_{p'}) \, J^{\,2}_{\ell}((\omega_{p'} - \omega_{\xi})\hat{\tau}). \tag{2.10}$$

Simple numerical comparison of both formulas describing the effective impedance, Eqs.(2.9) and (2.10), shows clearly that there is very little difference between both models.

3. EFFECTIVE IMPEDANCE

Further consideration will be confined to the real part of the impedance only, since the imaginary part does not enter explicitly into the growth-time formulae given by Eqs.(2.8) and (2.9). In order to evaluate the effective impedance one has to convolute the above four contributions to the transverse impedance with the beam spectrum according to Eqs.(2.9) and (2.10). Several lower harmonics of the beam spectrum are illustrated in Figure 1. The result of the above summation obviously depends on chromaticity.

One can notice that the relevant part of the transverse impedances, $Z_\perp(\omega)$, should have a diffraction-like character; a principal maximum of width $\lambda = \pi c/L$ at the origin and a series of equally spaced secondary maxima governed by the same width. Similarly, the harmonics of the beam spectrum, $\rho^{\ell}(\omega - \omega_\xi)$, have one ($\ell = 0$) or a pair ($\ell \geq 1$) of principal maxima of width $\varepsilon = \pi/2\hat{\tau}$ followed by a sequence of secondary maxima (See Figure 1). Both spectra are sampled by a discrete set of frequencies, $\omega_p = (p + \nu)\omega_o$. In case of relatively long proton bunches in the Tevatron at 150 GeV ($2\hat{\tau} = 2$–3×10^{-9} sec) both widths λ and ε are comparable and they are of the order of the chromatic frequency, ω_ξ, evaluated at about 10 units of chromaticity. These features combined with the convolution formula for the effective impedance, Eqs.(2.9) and (2.10), result in substantial 'overlap' of the transverse impedance and the beam spectrum, which in turn leads to large values of effective impedance for relatively small chromaticities ($\xi \sim 10$).

In contrast, the effective impedance evaluated with the broad-band part of the transverse impedance is much smaller than the previously discussed one. The last statement can be explained as follows; the width of the broad-band impedance peak, $\delta = \omega_c/Q$, is much larger than ε and in order to overlap this broad peak with the principal maximum of the power spectrum harmonics (to get a nonzero effective impedance) one would have to shift both spectra by ω_ξ of the order of δ. This, in turn, would require enormous values of the chromaticity ($\xi \sim 10^4$).

Summarizing, only the diffraction-like contributions to the transverse impedance are relevant to the discussed coherent betatron instability. A closed analytic expression for the inverse growth-time of the slow head-tail modes, ℓ, driven by a general peaked impedance will be derived in detail in the next section.

4. CHARACTERISTIC GROWTH TIME

From the discussion of Section 3 we identified the relevant contribution to the transverse coupling impedance. The transverse coupling impedance may be expressed analytically as follows[4]

$$\mathrm{Re}\, Z_\perp(\omega) = \frac{Z_0 L}{4ab}\, \frac{1}{\omega}\, \left(1 - \cos\frac{\omega L}{c}\right) \, , \tag{4.1}$$

where L is the length and a, b are the transverse sizes of the resonant structure, Z_0 is the characteristic shunt impedance. We are only concerned with the real part of the impedance which enters into the growth-time formula, Eq(2.8) and (2.9). As mentioned before, $Z_\perp(\omega)$ has a diffraction-like character; a principal maximum of width $\lambda = \pi c/L$ at the origin and a series of equally spaced secondary maxima governed by the same width. Similarly the beam power spectrum harmonics, $\rho^\ell(\omega - \omega_\xi)$, have one ($\ell = 0$) or a pair ($\ell \geq 1$) of principal maxima of width $\varepsilon = \pi/2\hat{\tau}$ followed by a sequence of secondary maxima. Both spectra are sampled by a discrete set of frequencies given by

$$\omega_p = (p + \nu)\omega_0 \, . \tag{4.2}$$

In the limit of $\varepsilon, \lambda \ll \omega_0$ the variable ω_p gains continuous character on the scale of the structure of both functions. This allows to replace the infinite summation in Eq.(2.9) by the integration according to the following substitution

$$\sum_{p=-\infty}^{\infty} \ldots \rightarrow \int_{-\infty}^{\infty} dp \ldots \tag{4.3}$$

Using specific impedance, given by Eq.(4.1) one can carry out the above integration and evaluate Z^ℓ_{eff} in closed analytic form. First, one can simplify ρ^ℓ, expressed by Eq.(2.4), by applying the substitution defined by Eq.(4.3) to the sum in the denominator and integrating it explicitly. The resulting expression has the following form

$$\rho^{\ell}(\omega) = \frac{\hat{\tau}}{2\pi\omega_o} h_{\ell}(\omega) \quad ,$$

where (4.4)

$$h_{\ell}(\omega) = \frac{4}{\pi^2} (\ell + 1) \frac{1 + (-1)^{\ell} \cos(2\omega\hat{\tau})}{[(2\omega\hat{\tau}/\pi)^2 - (\ell + 1)^2]^2} .$$

Substituting Eqs.(4.1) and (4.4) in Eq.(2.4) allows to rewrite the effective impedance in terms of the following integral

$$\mathcal{Z}^{\ell}_{\mathrm{eff}} = \frac{Z_o c(\ell + 1)}{\omega_o ab} \frac{\pi^2}{16} J^{\ell} \quad ,$$

where (4.5)

$$J^{\ell} = \int_{-\infty}^{\infty} d\omega \, \frac{[1 - \cos(\omega + \omega_{\xi}) \lambda] \, [1 + (-1)^{\ell} \cos(2\omega\hat{\tau})]}{(\omega + \omega_{\xi})(\omega + \alpha)^2(\omega - \alpha)^2}$$

and

$$\alpha = \frac{\pi(\ell + 1)}{\hat{\tau}} \quad .$$

Here ω_{ξ} and α define poles in the complex ω-plane connected with the chromatic phase shift and beam spectrum respectively. The integral J^{ℓ} can be expressed in terms of much simpler integrals defined by

$$J^{+}(t)= \int_{-\infty}^{\infty} d\omega \, \frac{\cos(\omega t)}{(\omega + \omega_{\xi})(\omega + \alpha)^2(\omega - \alpha)^2} \, ,$$

$$J^{-}(t)= \int_{-\infty}^{\infty} d\omega \, \frac{\sin(\omega t)}{(\omega + \omega_{\xi})(\omega + \alpha)^2(\omega - \alpha)^2} \, , \tag{4.6}$$

in the following form

$$J = J^{+}(0) + (-1)^{\iota} J^{+}(2\hat{\tau})$$

$$+ \cos(\omega_{\xi}\lambda) \left[(-1)^{\iota} \frac{J^{+}(\lambda + 2\hat{\tau}) + J^{+}(\lambda - 2\hat{\tau})}{2} - J^{+}(\lambda) \right] \tag{4.7}$$

$$- \sin(\omega_{\xi}\lambda) \left[(-1)^{\iota} \frac{J^{-}(\lambda + 2\hat{\tau}) + J^{-}(\lambda - 2\hat{\tau})}{2} - J^{-}(\lambda) \right] .$$

Both integrals given by Eq.(4.6) can be easily converted into contour integrals in the complex ω-plane and evaluated through Cauchy's integral theorem. The result is given below

$$J^{+}(t) = \frac{\pi \sin(\omega_{\xi} t)}{(\omega_{\xi}^2 - \alpha^2)^2} - \frac{\pi \omega_{\xi} t}{2\alpha^2} \frac{\cos(\alpha t)}{\omega_{\xi}^2 - \alpha^2} + \frac{\pi \omega_{\xi}(\omega_{\xi}^2 - 3\alpha^2)}{2\alpha^3(\omega_{\xi}^2 - \alpha^2)^2} \sin(\alpha t)$$

$$J^{-}(t) = \frac{\pi \cos(\omega_{\xi} t)}{(\omega_{\xi}^2 - \alpha^2)^2} + \frac{\pi t \sin(\alpha t)}{2\alpha(\omega_{\xi}^2 - \alpha^2)} - \frac{\pi \cos(\alpha t)}{(\omega_{\xi}^2 - \alpha^2)^2} \, . \tag{4.8}$$

Final substitution of Eqs.(4.5)–(4.8) into Eq.(2.4) leads after a tedious algebra to a simple closed formula describing the growth-time of the ℓ-th head-tail mode given below

$$\frac{1}{\tau^{\ell}} = \frac{ceI_0\beta}{4\pi\nu\gamma m_0} \; \frac{Z_0 R\pi^2}{ab} \; \frac{\pi(\ell+1)}{\chi^2 - \pi^2(\ell+1)^2} \times$$

$$\left[\frac{\chi}{2\pi^2(\ell+1)^2} + (-1)^{\ell} \frac{\sin\chi}{\chi^2 - \pi^2(\ell+1)^2} \right] . \tag{4.9}$$

Here $\chi = 2\frac{\xi}{\eta}\,\omega_0\hat{\tau}$, is the betatron phase shift between the head and tail of the bunch.

5. NUMERICAL EXAMPLE

At this point some comparison between numerical results of our model with the observed coherent instability is in order. As the example we will use the Tevatron at 150 GeV, with the bunch intensity of 1.8×10^{10}ppb. The observed growth-time was fast; less than 30×10^{-3}sec. Typically, the full ring would go unstable, but we have observed unstable behavior in a partial azimuth of the ring when bunches of significantly higher intensity were present.

Assuming only one dominant contribution to the transverse coupling impedance; kicker magnets, the inverse growth-time was calculated numerically according to Eqs.(2.8)–(2.10) and (4.9) with: L = 1 m, a = 3.7 cm, b = 1.9 cm and Z_o = 377 Ohm (Tevatron's kicker magnets). The resulting growth-rates as a function of chromaticity evaluated for different slow head-tail modes (ℓ = 0, 1, 2, 3) are illustrated in Figure 2. One can immediately see a qualitative difference between the $\ell = 0$ and $\ell \geq 1$ modes.

The experimentally observed situation corresponds to chromaticity of about 3 units. Figure 2 shows that $\ell = 1$ mode is strongly unstable with the growth-time of about 20×10^{-3}sec, which would suggest that this mode is responsible for the observed betatron instability. One way of suppressing the $\ell = 1$ mode would be by decreasing chromaticity. However, as one can see from Figure 2, the $\ell = 0$ mode appears to be unstable for negative chromaticities and might lead to significant enhancement of coherent betatron motion. Fortunately, this potentially offending mode can be effectively suppressed by the active damper system. This efficient cure for the $\ell = 0$ mode obviously does not work in case of the higher modes, since its feedback system picks up only the transverse position of a bunch centroid, which remains zero due to the symmetry of the higher modes[6]. Another possible cure (also effective for the $\ell \geq 1$ modes) would involve the Landau damping through the octupole-induced betatron tune spread. Increasing betatron amplitude of initially unstable mode causes increase of the tune spread, which will eventually self-stabilize development of this mode.

6. SUMMARY

In conclusion, we presented a systematic formalism describing coherent betatron instability driven by a peaked impedance. The resulting closed formula for the characteristic growth-time vs chromaticity is practically equivalent to quite complex Vlasov equation based results, which do not have nice numerical simplicity of our formula. Furthermore, there is a good agreement between the characteristic growth-times coming from the measurement and those calculated within the framework of the presented model .

REFERENCES

1) F. Sacherer, Proc. 9-th Int. Conf. on High Energy Accelerators, Stanford 1974, p. 347.

2) S. Krinsky and J.M. Wang, Particle Accelerators **17**, 109 (1985).

3) F. Sacherer, CERN/SI-BR/72-5 (1972), unpublished.

4) K.Y. Ng, Principles of the High Energy Hadron Colliders, Part I: The SSC, edited by A.W. Chao and M. Month, American Institute of Physics 1987.

5) J. Gareyte and F. Sacherer, Proc. 9-th Int. Conf. on High Energy Accelerators, Stanford 1974, p. 341.

6) L.J. Laslett, V.K. Neil, A.M. Sessler, Rev. Sci. Instr., **36**, (1965), p. 436.

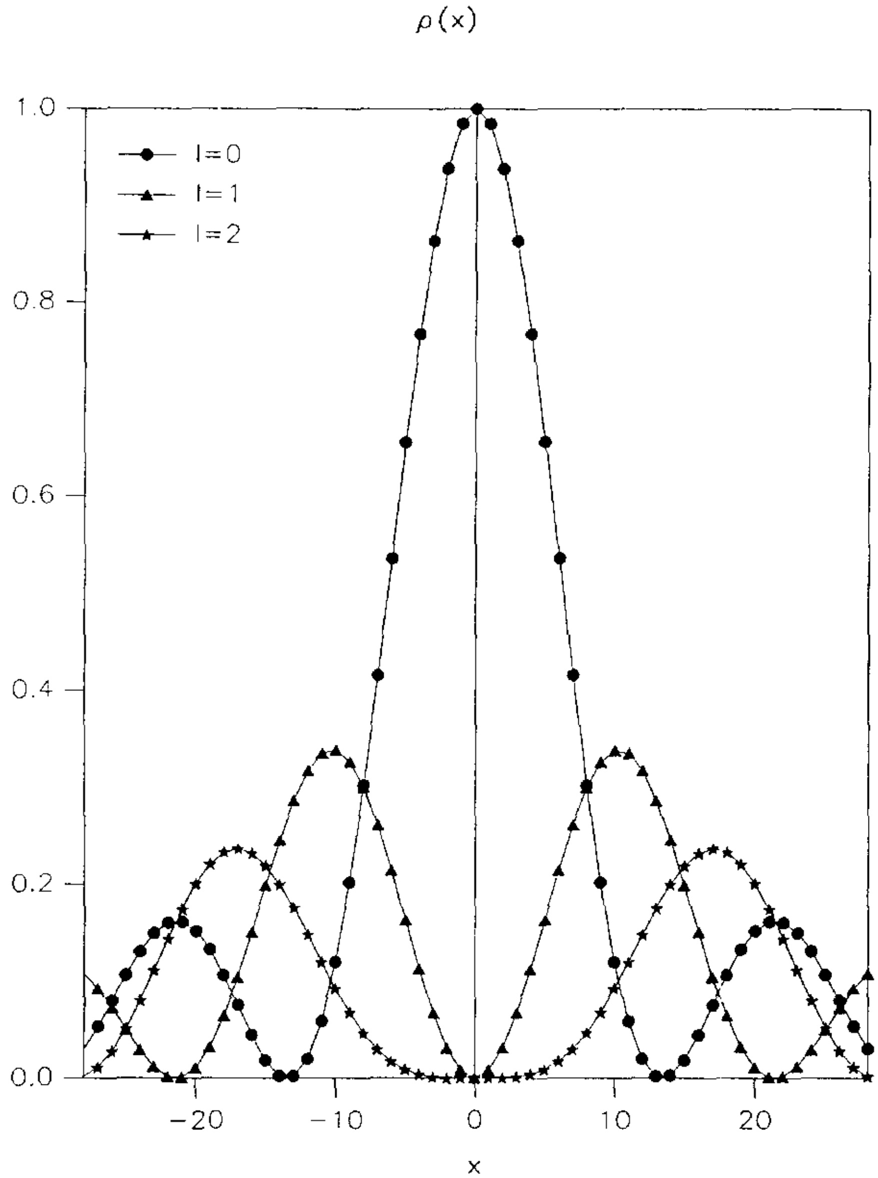

Figure 1 Harmonics of the beam power spectrum $\rho^{\ell}(\omega)$. Markers denote the sampling frequencies $\omega_p = \omega_o(Mp + \nu)$. Dimensionless frequency is given in units of $x = \frac{\omega}{M\omega_o}$

Tevatron (fixed target) p-injection @ 150 GeV

ε = 1.5 eV-sec.

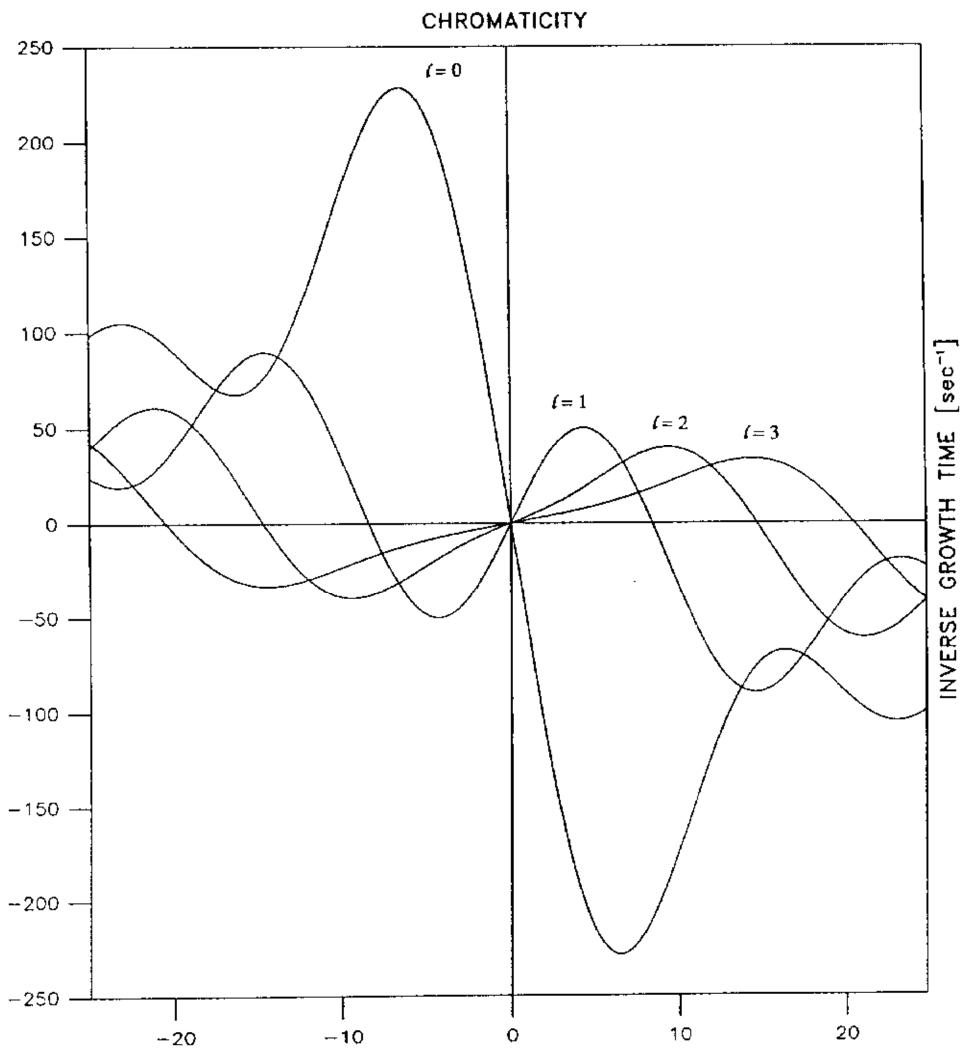

Figure 2 A family of inverse growth-time vs chromaticity curves evaluated numerically for various head-tail mode indices ℓ